Longitudinal [18F]FDG PET-MRI at 9.4 Tesla in Twitcher mice using spatial normalization

Poonam Choudhary[1,2], Akshay V Dhamankar[1], Nadav Weinstock[3,4], Cheryl Knapp[6], Marilena Preda[1,6], Daesung Shin[3,4], Robert Zivadinov[1,6], Lawrence Wrabetz[1,3,5], Ferdinand Schweser[1,6]

[1]Buffalo Neuroimaging Analysis Center, Department of Neurology; [2]Department of Medical Physics; [3]Hunter James Kelly Research Institute; [4]Department of Biochemistry; [5]Department of Neurology
[6]Center for Biomedical Imaging at the Clinical and Translational Science Institute
Jacobs School of Medicine and Biomedical Sciences at the University at Buffalo, The State University of New York

Buffalo Neuroimaging Analysis Center
MRI Biophysics Lab

University at Buffalo

INTRODUCTION

- PET-MRI benefits from the complementary information provided by the two modalities, setting the stage for truly novel imaging approaches that are currently being explored, such as the use of dual-modality tracers,[1] the correction of motion effects in PET based on real-time MR information,[2] and advanced MRI techniques that complement PET.[3,4]
- Krabbe Disease is a rare genetic disorder leading to demyelination and death of affected child within early years of birth. Hematopoietic stem cell transplantation (HCST), the only treatment available, leaves us with very limited opportunities to diagnose the disease at an early stage.
- Preclinical PET-MRI, is only gradually leaving the proof-of-concept stage, which may be explained by technical difficulties due to the size-constraints (bore diameter of often <30 cm) and the particularly high magnetic field strength needed for preclinical MRI (>7T).
- In this study, we present initial results of a first *in vivo* application of 18F-Fludeoxyglucose (FDG) PET-MRI at 9.4 Tesla in the Twitcher mouse model of Krabbe disease, in which an altered pre-symptomatic glucose metabolism had been suggested by metabolomics.[5]

PET-MRI SETUP

The employed prototype PET detector ring was provided by SynchroPET, Inc. (Stony Brook, NY).[6] It is comprised of 12 radially oriented scintillator crystals (LYSO, 18.5x9.6x6mm^3, 4x8 pixels) and avalanche photodiodes (APD, 415V) resulting in 44mm/80mm inner/outer shell diameters and a depth of 25mm. We used a 20 cm diameter horizontal-bore 9.4 Tesla magnet (Biospec 94/20 USR, Bruker Biospin) equipped with a standard imaging gradient coil (inner diameter 11.4cm), and a quadrature volume transceiver coil (inner/outer diameter 23/44mm). An in-house built modular holder was used for the PET camera, RF coil, and anesthesia/monitoring equipment as shown in **Fig. 1**.

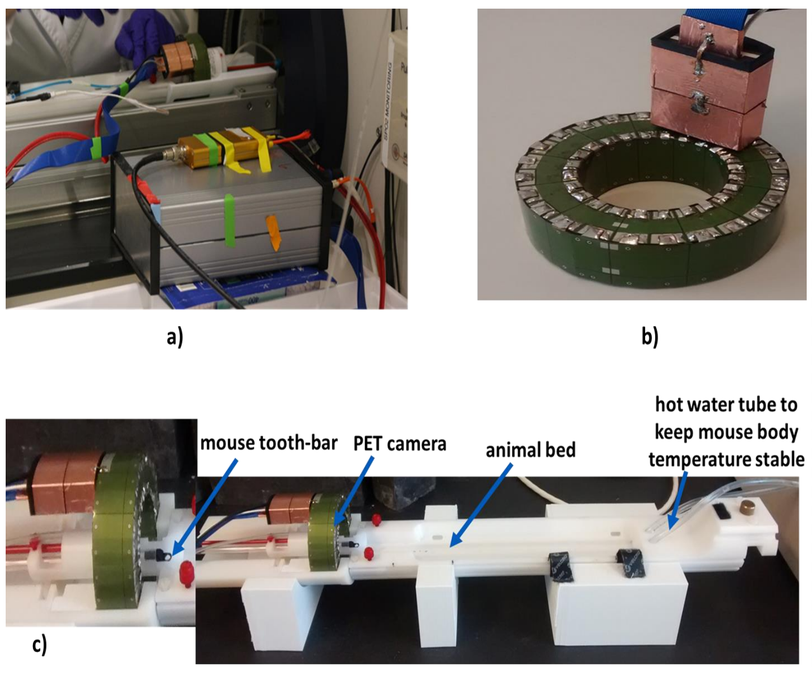

Figure 1: Overview of the modular experimental setup for simultaneous PET-MRI at 9.4 Tesla. (a) Animal bed with installed miniature PET detector in front of the magnet bore during animal positioning. (b) PET detector with the electromagnetic shield in green. (c) Custom 3D printed modular integration set up of the PET ring.

EXPERIMENTAL DESIGN

- The local radiation safety committee approved the experimental procedures, and all procedures involving animals were performed according to the guidelines of Institutional Animal Care and Use Committee (IACUC).
- Twitcher mice (Twi) were maintained on the background of C57BL/6N purchased from Charles River Laboratories (Kingston, PA). We enrolled 7 Twi and 7 wild-type (wt) animals.
- We injected the mice at postnatal (P) day 15 (P15; pre-symptomatic), P21 (just prior to first symptoms), and P28 (structural and behavioral changes) with 100µl of ^{18}F-FDG, 250±95µCi. After 20 minutes of awake uptake time under a heat lamp, mice were anesthetized with Isoflurane and positioned on the animal bed in the magnet room.
- PET scanning started 30 minutes after the injection and continued for up to 60 minutes. *Simultaneously*, we acquired axial T2-RARE and T1-RARE images with MRI.

IMAGE RECONSTRUCTION AND CO-REGISTRATION

We reconstructed PET images every 60 seconds on a 0.24x0.24x0.29mm^3 grid using an iterative 3D maximum likelihood-expectation maximization (MLEM) algorithm with 3D spline-based spatial filtering. PET image intensities were decay-corrected to the injection time, augmented with animal body weight, and normalized relative to the injected dose.

Corrected PET images were fully automatically registered to the T2-RARE images based on a separate coordinate-system calibration experiment (**Fig. 2a**).

SPATIAL NORMALIZATION

We normalized the T2 images to a custom template (**Fig. 2b**) calculated from all T2 scans with ANTS, and applied the resulting deformation fields to the T2-registered PET images. A subsequent iterative rigid-body registration of all PET images to the cohort-average mitigated the impact of detector positioning inaccuracies.

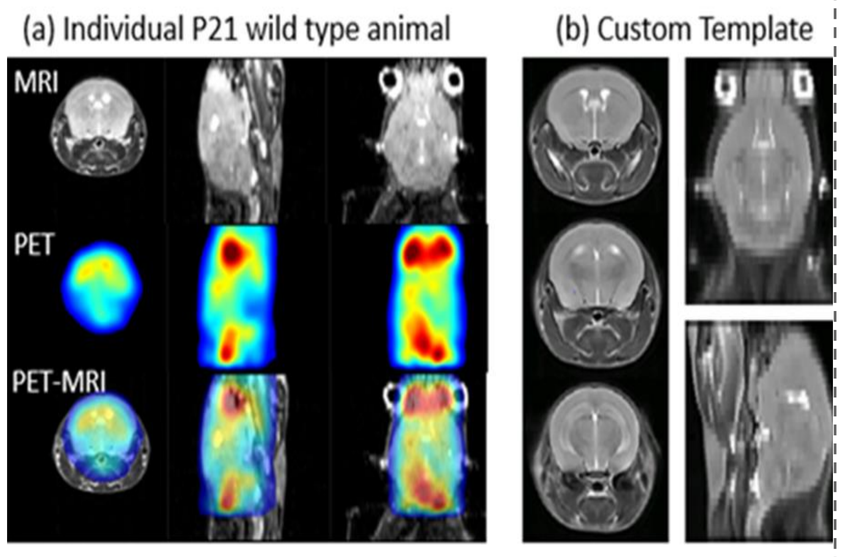

Figure 2. (a) T2 weighted MRI, PET, PET overlaid on T2-MRI. (b) Sagittal, coronal, and three axial views of the common T2-template.

ATLAS-BASED ANALYSIS

We registered the Brookhaven National Laboratory (BNL) C57BL Mouse Atlas to the custom T2 template using ANTs (**Fig. 3**) and assessed the average regional FDG uptake in major brain regions and in the whole brain.

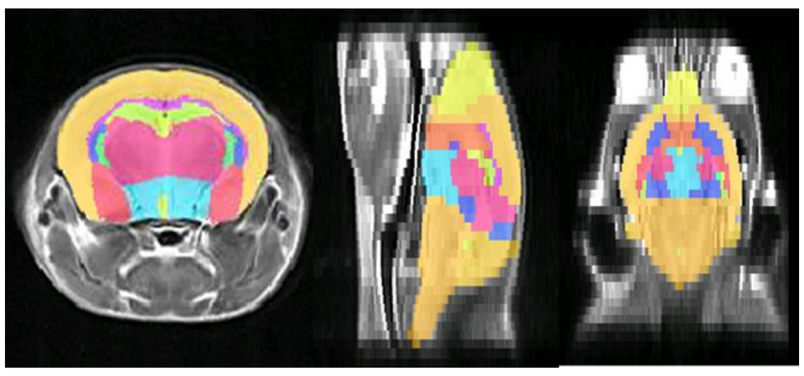

Figure 3. Axial, Sagittal, and coronal views of a BNL labels registered to our T2-MRI template.

RESULTS

Two Twi and one wt did not survive the experiments or their data did not pass quality control at P21 and P28, respectively.

Figure 4 shows the group average whole-brain FDG uptake. Both wt (p<0.01) and Twi (p=0.02) showed significantly decreasing FDG uptake from P15 to P21, which then stablized (p>0.2). Whole brain uptake was similar between groups at all time points (p>0.2).

Figure 5 summarizes the regional analyses. The highest uptake was seen in both groups at P15 in the Thalamus and in the olfactory lobes at P21 and P28. Uptake was not significantly different in any of the regions between groups at P15 and P28 (p>0.12). Differences reached significance at P21 in the cortex (p=0.02), where it was reduced in Twi compared to wt.

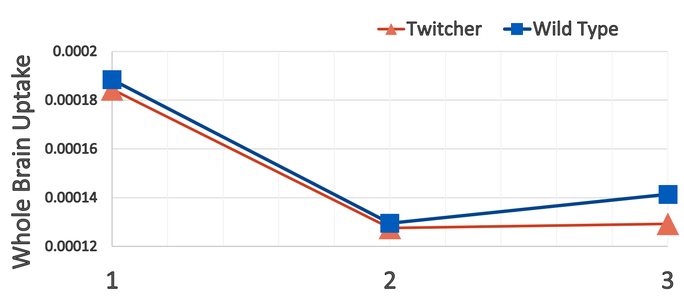

Figure 4. Group average whole brain FDG uptake in Twitcher and wild type animals at the three different time points (P15, P21, P28).

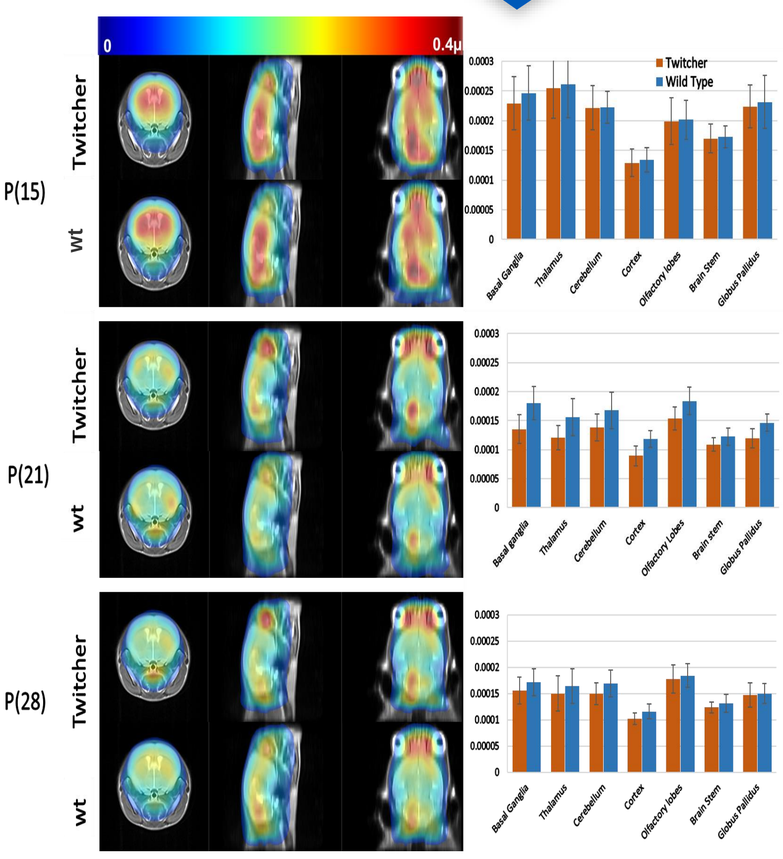

Figure 5. Left: Axial, sagittal and coronal views of the group average FDG regional uptake in template space. Right: Regional uptake in the 7 largest brain regions. Error bars indicate 95% confidence intervals.

DISCUSSION AND CONCLUSION

- We have demonstrated the feasibility of *in vivo* longitudinal PET-MRI at 9.4T to quantify regional glucose metabolism in mouse pups and during maturation. MRI enabled a regional analysis of brain PET images via spatial normalization.
- The highly similar glucose uptake patterns at P15 for both groups demonstrated the reproducibility and stability of the experimental setup.
- Decreasing glucose uptake with brain maturation is consistent with previous reports of decreasing uptake during the transition from adolescence to adulthood.[8]
- Twitcher animals showed decreased uptake at P21 but differences reached significance only in the cortex. These results are in line with a previously suggested disturbance of glucose metabolism in Krabbe disease.[5]
- Limitation of our study are the small number of animals and differences in body-weight between the groups (in particular at P28) that render the commonly-used mass-based normalization of uptake values problematic. Twi and wt animals did not differ significantly in weight at P15 (p=0.5; Twi: 5.61±0.38g, wt: 5.61±0.40g), but at P21 (p=0.018; Twi: 6.72±0.79g, wt: 8.49±1.47g) and P28 (p<0.001; Twi: 9.00±0.70g, wt: 13.6±2.2g).
- The effect of body weight differences will have to be studied in more detail. A more detailed statistical analysis may exploit the longitudinal nature of the data and account for differences in baseline blood glucose levels.

Acknowledgements

This work was supported in part by the University at Buffalo Center for Advanced Biomedical and Bioengineering Technology (UB CAT), by the National Center for Advancing Translational Sciences of the National Institutes of Health under award Number UL1TR001412 and by an equipment grant from SynchroPET Inc. The content is solely the responsibility of the authors and does not necessarily represent the official views of the NIH. The authors are grateful to Nicola Bertolino for his support with the design of the experimental setup. Also, we thank Drs. D. Schlyer, S.D. Smith for scientific guidance and inspiration, and Y. Sinelnikov, D. Hertz, and M. Hamburger for their professional attitude and support to this project.

References

[1] S. Y. Chun, T. G. Reese, J. Ouyang, B. Guerin, C. Catana, X. Zhu, N. M. Alpert, and G. El Fakhri, "MRI-Based Nonrigid Motion Correction in Simultaneous PET/MRI," Journal of Nuclear Medicine, vol. 53, no. 8, pp. 1284–1291, 2012.
[2] T. Stadhouders, A. Savio, J. Diehl-Schmid, C. Sorg, T. Grimmer, and I. Yakushev, "Alterations in neurocognitive networks in dementing disorders as assessed with simultaneous PET/fMRI," J. Nucl. Med., vol. 57, no. supplement_2, pp. 237–, may 2016.
[3] S. Bisdas, R. Ritz, B. Bender, C. Braun, C. Pfannenberg, M. Reimold, T. Naegele, and U. Ernemann, "Metabolic Mapping of Gliomas Using Hybrid MR-PET Imaging: Feasibility of the Method and Spatial Distribution of Metabolic Changes." Investigative Radiology, vol. 00, no. 00, pp. 1–7, 2013.
[4] K. Simonyan, P. Herscovitch, and B. Horwitz, "Speech-induced striatal dopamine release is left lateralized and coupled to functional striatal circuits in healthy humans: A combined PET, fMRI and DTI study," NeuroImage, vol. 70, pp. 21–32, 2013.
[5] N. I. Weinstock et al, "Metabolic profiling reveals biochemical pathways and potential biomarkers associated with the pathogenesis of Krabbe disease,"Journal of Neuroscience Research on 94 (2016): 1094–1107.
[6] N. Bertolino et al, "Integrated setup and characterization of an MRI-compatible PET camera for preclinical ultra-high field imaging," Proc Intl Soc Mag Reson Med on 25 (2017): 4087
[7] Jannis Hanspach et al, "Methods for the Computation of Templates From Quantitative Magnetic Susceptibility Maps (QSM): Toward Improved Atlas- and Voxel-Based Analyses (VBA)," J Magn Reson Imaging, on 46(5) 2017: 1474-1484
[8] Harry Chugani A Critical Period of Brain Development: Studies of Cerebral Glucose Utilization with PET,"Preventive Medicine, on 27(2) 1998:184-18

7th Conference on PET/MR and SPECT/MR
May 20-23, 2018; La Biodola, Isola d'Elba, Italy
Corresponding author: P. C. (poonamch@buffalo.edu)
Session 8 , Board:13
Presentation time: Wednesday, 16:00 – 17:30

mbl.bnac.net